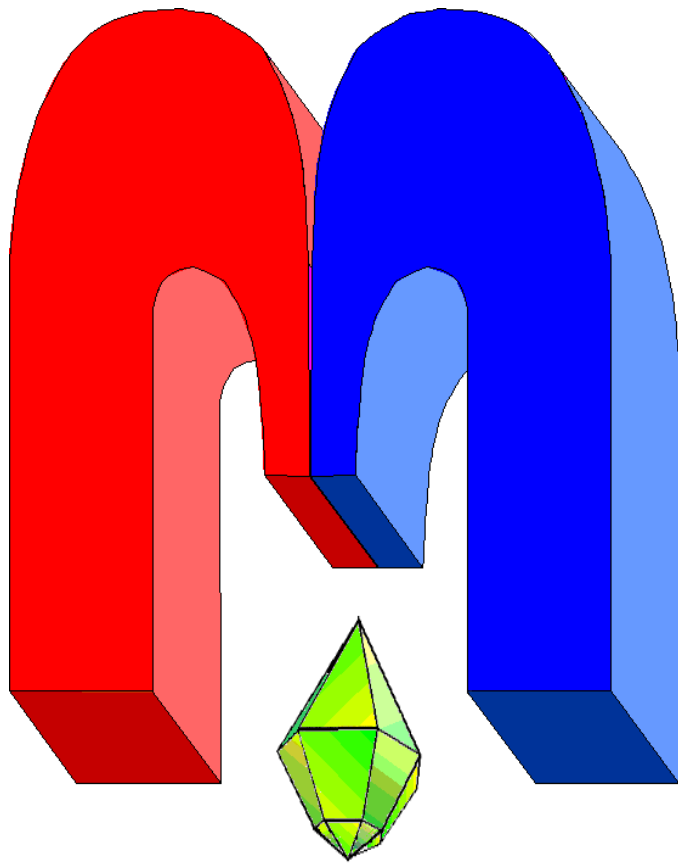


ISSN 2072-5981
doi: 10.26907/mrsej



***Magnetic
Resonance
in Solids***

Electronic Journal

Volume 26

Issue 2

Article No 24215

1-17 pages

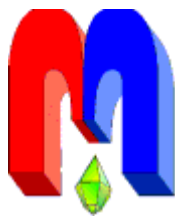
June, 6

2024

doi: 10.26907/mrsej-24215

<http://mrsej.kpfu.ru>

<https://mrsej.elpub.ru>



Established and published by Kazan University*
Endorsed by International Society of Magnetic Resonance (ISMAR)
Registered by Russian Federation Committee on Press (#015140),
August 2, 1996
First Issue appeared on July 25, 1997

© Kazan Federal University (KFU)†

"Magnetic Resonance in Solids. Electronic Journal" (MRSej) is a peer-reviewed, all electronic journal, publishing articles which meet the highest standards of scientific quality in the field of basic research of a magnetic resonance in solids and related phenomena.

Indexed and abstracted by
Web of Science (ESCI, Clarivate Analytics, from 2015), Scopus (Elsevier, from 2012), RusIndexSC (eLibrary, from 2006), Google Scholar, DOAJ, ROAD, CyberLeninka (from 2006), SCImago Journal & Country Rank, etc.

Editor-in-Chief

Boris **Kochelaev** (KFU, Kazan)

Honorary Editors

Jean **Jeener** (Universite Libre de Bruxelles, Brussels)

Raymond **Orbach** (University of California, Riverside)

Executive Editor

Yurii **Proshin** (KFU, Kazan)

mrsej@kpfu.ru



This work is licensed under a [Creative Commons Attribution-ShareAlike 4.0 International License](https://creativecommons.org/licenses/by-sa/4.0/).

 This is an open access journal which means that all content is freely available without charge to the user or his/her institution. This is in accordance with the [BOAI definition of open access](https://www.boai.ru/).

Technical Editors

Maxim **Avdeev** (KFU, Kazan)
Vadim **Tumanov** (KFU, Kazan)
Fail **Sirayev** (KFU, Kazan)

Editors

Vadim **Atsarkin** (Institute of Radio Engineering and Electronics, Moscow)

Yurij **Bunkov** (CNRS, Grenoble)

Mikhail **Eremin** (KFU, Kazan)

David **Fushman** (University of Maryland, College Park)

Hugo **Keller** (University of Zürich, Zürich)

Yoshio **Kitaoka** (Osaka University, Osaka)

Boris **Malkin** (KFU, Kazan)

Alexander **Shengelaya** (Tbilisi State University, Tbilisi)

Jörg **Sichelschmidt** (Max Planck Institute for Chemical Physics of Solids, Dresden)

Haruhiko **Suzuki** (Kanazawa University, Kanazawa)

Murat **Tagirov** (KFU, Kazan)

Dmitrii **Tayurskii** (KFU, Kazan)

Valentine **Zhikharev** (KNRTU, Kazan)

Invited Editor of Special Issue[‡]: Eduard Baibekov (KFU, Kazan)

* Address: "Magnetic Resonance in Solids. Electronic Journal", Kazan Federal University; Kremlevskaya str., 18; Kazan 420008, Russia

† In Kazan University the Electron Paramagnetic Resonance (EPR) was discovered by Zavoisky E.K. in 1944.

‡ Dedicated to Professor Boris Z. Malkin on the occasion of his 85th birthday

Dimer self-organization of impurity rare earth ions in forsterite (Mg_2SiO_4) single crystals as revealed by EPR spectroscopy[†]

V.F. Tarasov

Zavoisky Physical-Technical Institute,
FRC Kazan Scientific Center of RAS, Kazan 420029, Russia

*E-mail: tarasov@kfti.knc.ru

(Received May 16, 2024; accepted May 30, 2024; published June 6, 2024)

Electron paramagnetic resonance is one of the most informative methods for studying the local structure and magnetic properties of impurity paramagnetic centers in crystals. This mini-review presents the results of a study of paramagnetic centers formed by rare earth ions Ho^{3+} , Tm^{3+} , Er^{3+} and Yb^{3+} in single crystals of synthetic forsterite (Mg_2SiO_4). The structural features and magnetic properties of the studied centers are presented. It was found that a well-pronounced effect of dimer self-organization is observed for impurity trivalent ions in forsterite. As a result, concentration of dimer associates significantly exceeds the concentration expected with a statistically uniform distribution of impurity ions across the nodes of the crystal lattice.

PACS: 76.30.Kg, 75.30.Hx, 75.30.Gw, 71.70.Ej.

Keywords: Electron paramagnetic resonance, rare earth ions, forsterite, dimer associates

1. Introduction

Electron paramagnetic resonance (EPR) is one of the most informative methods for studying the structure and magnetic properties of impurity paramagnetic centers in crystals. This article provides an overview of our work on the study by the EPR of single ions and dimer associates of impurity rare earth (RE) ions in forsterite (Mg_2SiO_4). Dimer associates (DA) of the RE ions in dielectric crystals are objects of the study for several reasons. An interesting property of these associates is cooperative up-conversion luminescence, when two ions of the dimer associate absorb two photons, and emit the single photon with a frequency exceeding the frequency of exciting photons. In the articles [1, 2], dimer associates of RE ions were considered as coupled qubits that can be used for implementation of elementary algorithms of quantum computations. With a small concentration (C) of impurity ions and their statistical distribution over the crystal lattice, the relative concentration of DA is proportional to C^2 , and it is much less than concentration of single ions (SI). However, in some cases, the statistical distribution of impurity ions in the crystal is disturbed, and impurity ions form the DA with concentration significantly exceeding the concentration expected with statistical distribution of the impurity ions. The physical origin of this effect is connected with the need to compensate excess cation charge arising during heterovalent substitution of a divalent lattice ion with a trivalent impurity ion. The cation charge remains unchanged when three divalent ions are substituted by the DA consisting of two trivalent impurity ions with a neighboring vacancy of a divalent ion. The similar effect was observed, in particular, for bromides (CsCdBr_3) for Gd^{3+} [3,4], Tb^{3+} [5], Nd^{3+} [6,7], Er^{3+} [8,9], Ho^{3+} [10] and Yb^{3+} [11,12] ions. In this case, trivalent ions replaced divalent cadmium ions in a quasi-one-dimensional chain of bromine octahedra directed along the crystallographic three-fold c -axis.

B.Z. Malkin was the initiator of our research of the dimer self-organization of impurity non-kramers Ho^{3+} and Tm^{3+} ions in CsCdBr_3 single crystals [13, 14]. The measurements were

[†]This paper is dedicated to Professor Boris Z. Malkin, who made a significant contribution to the field of magnetic radio spectroscopy in Kazan University, on the occasion of his 85th birthday.

carried out using the frequency tunable broadband EPR spectrometer [15]. It was found that Ho^{3+} and Tm^{3+} impurity ions in CsCdBr_3 have a pronounced tendency to self-formation of DA during crystal growth. Later, we observed a similar dimer self-organization of Cr^{3+} impurity ions substituting Mg^{2+} ions in forsterite single crystals [16,17]. All this prompted us to pay some attention for a search for the effect of dimer self-organization of trivalent impurity RE ions in forsterite single crystals.

2. Samples and Experiment Details

The forsterite crystal structure has orthorhombic symmetry with the Pbnm space group. A single crystal cell includes four Mg_2SiO_4 formula groups. Its dimensions are $a = 0.4762$ nm, $b = 1.0225$ nm and $c = 0.5994$ nm [18]. The structure is formed by a hexagonal dense packing of oxygen atoms, in which half of the octahedral positions are occupied by Mg^{2+} ions. These oxygen octahedra form a toothed chain oriented along the crystal c -axis. The unoccupied oxygen octahedra form similar chains, offset in the (bc) plane by $b/2$. The projections of the oxygen octahedra onto the (bc) plane are shown in Figure 1.

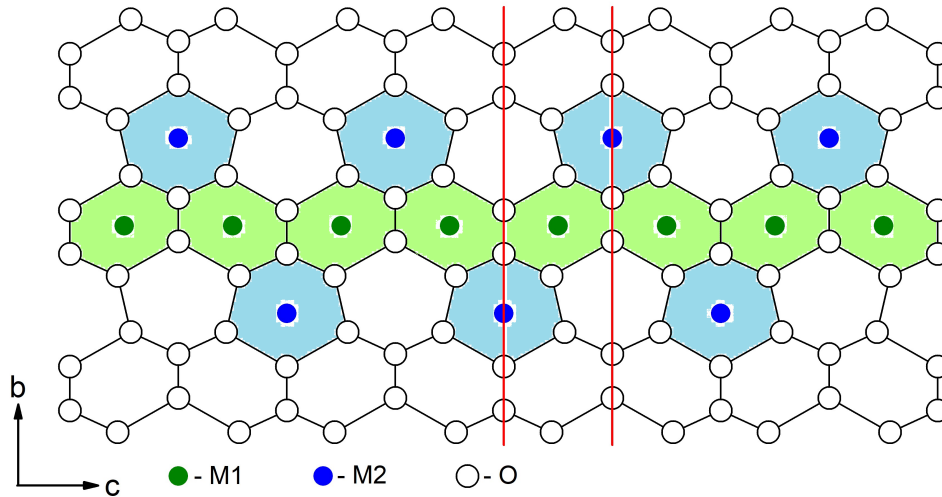


Figure 1. Projections of Mg_2SiO_4 oxygen octahedra onto the crystallographic bc plane. M1 and M2 octahedra are colored by green and blue, respectively.

Filled octahedra are highlighted with a colored background. There are (ab) planes of mirror symmetry in the forsterite crystal structure. The projections of these planes onto the (bc) plane are shown in Figure 1 with red lines. There is another layer of octahedra in the forsterite unit cell, offset by $a/2$ relative to the first one. Occupied octahedra of the second layer are placed above the unoccupied octahedra of the first layer. There are two crystallographic different types of oxygen octahedra. Magnesium positions in the occupied octahedra are denoted M1 and M2 sites. There are four Mg^{2+} ions in the M1 and M2 sites. The crystal field at the M1 site has inversion symmetry with the point group C_i . Magnesium ions in the M2 site lie in mirror planes. The crystal field in this position has mirror symmetry with the point group C_s . For an impurity ion in the M2 site, mirror symmetry requires that one of the principal magnetic axes coincides with the crystallographic c -axis, and the other two axes lie in the (ab) plane. The ratio of inversion symmetry with respect to the magnetic field for two M2 centers located in different (ab) planes requires their pairwise magnetic equivalence. Therefore, for an arbitrary orientation of the magnetic field, there are two magnetically nonequivalent ions at the M2 sites located

in different (*bc*) planes. There are four magnetically nonequivalent centers for impurity ions substituting magnesium in the M1 sites. The principal magnetic axes of these centers should be symmetrical with respect to the mirror (*ab*) plane. This qualitative difference in the orientation of the principal magnetic axes makes it possible to unambiguously determine the position of the impurity ion from orientational dependencies of EPR spectra.

This article presents the results of our study of the structure and magnetic properties of paramagnetic centers formed by impurity Ho^{3+} , Tb^{3+} , Er^{3+} and Yb^{3+} ions in forsterite by continuous wave EPR spectroscopy. Ho^{3+} and Tb^{3+} ions have integer total electron magnetic moment, and in the low-symmetry forsterite crystal field the electron states of the ground multiplets of these ions split into singlet levels. The frequency of resonance transitions between these levels may significantly exceed the operation frequency of commercial EPR spectrometers. Therefore, study of these ions was carried out on a broadband spectrometer operating in the frequency range of 64–535 GHz [15]. Kramers Er^{3+} and Yb^{3+} ions with half-integer total magnetic moment were studied using commercial spectrometers ELEXYS E580 and ELEXYS E680. All measurements were carried out at cryogenic temperatures. Samples were grown by the Chokhralsky method from a melt with a content of impurity RE ions of 2–10 wt.%. The distribution coefficient of impurity trivalent RE ions between the forsterite crystal and melt does not exceed 10^{-2} [19]. Therefore, the concentration of impurity RE ions in our samples was less than 10^{-3} .

3. Ho^{3+} ions

The ground state of Ho^{3+} ion with $4f^{10}$ electron configuration is $^5\text{I}_8$. The nuclear spin of ^{165}Ho (the 100% abundance) $I = 7/2$. Thus, the hyperfine structure (HFS) of EPR spectra of the Ho^{3+} SI should consist of 8 lines corresponding to “allowed” transitions without changing the projection of the nuclear spin I_z on the quantization axis. For a holmium dimer associate, the HFS should consist of 64 “allowed” transitions. Impurity centers of the Ho^{3+} ions in forsterite were studied in the articles [20, 21]. Examples of the Ho^{3+} SI and DA spectra are shown in Figure 2. The SI spectrum contains 8 hyperfine components. The 64 hyperfine components of the DA are overlapped. Therefore, the HFS for each transition between two electron levels of the DA consists of 8 groups of lines with an irregular structure. Figure 3 shows the frequency-field dependencies of the observed transitions.

It follows from optical measurements and calculations of crystal field parameters [21] that the observed spectra correspond to resonance transitions between singlet levels of the ground electron quasi-doublets, and the energy of the other electron levels is more than 1000 GHz. Therefore, as a first approximation, it may be assumed that the states of the ground quasi-doublets of the Ho^{3+} impurity centers do not mix with the excited states. Then, for the non-Kramers ions, the $g_x = g_y = 0$ [22], and a simple effective spin Hamiltonian for effective electron spin $S = 1/2$ can be used to describe the frequency-field dependencies of the resonance transitions [23].

$$H_{\text{eff}} = \Delta S_x + g_z \mu_B B_z S_z + A_z I_z S_z, \quad (1)$$

Here, the first term corresponds to the zero field splitting between electron levels, the second term corresponds to the electron Zeeman energy, the third term corresponds to the hyperfine interaction between the effective electron spin $S = 1/2$ and the nuclear spin $I = 7/2$. Energies of the electron-nuclear levels in this case may be calculated analytically

$$W = \pm \frac{1}{2} \sqrt{(g_z \mu_B B_z + A_z I_z)^2 + \Delta^2}. \quad (2)$$

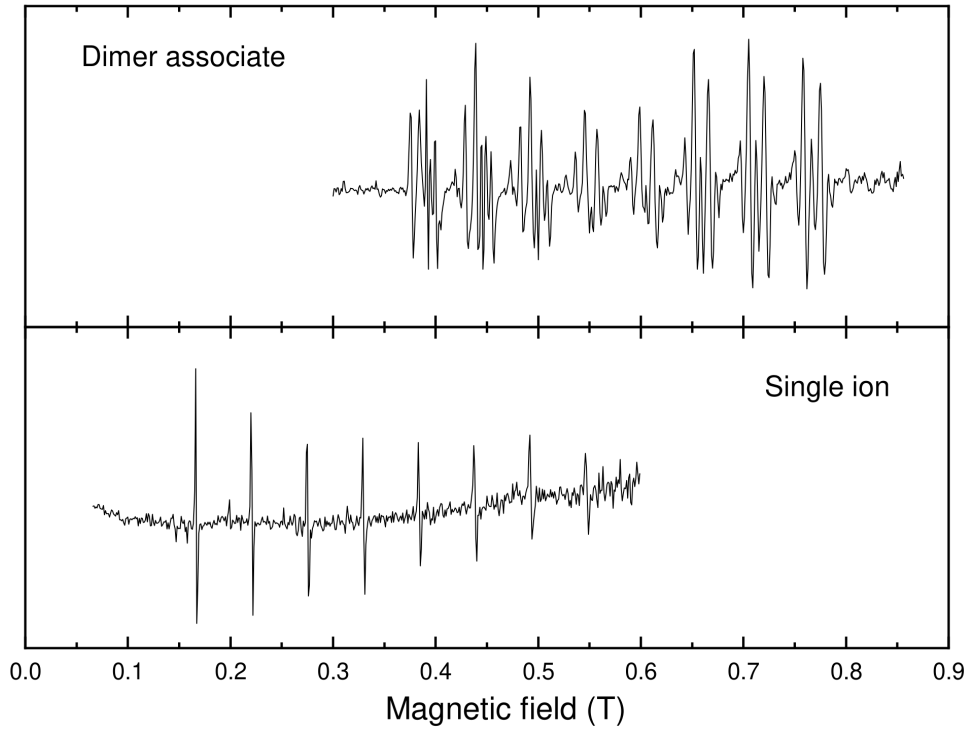


Figure 2. EPR spectra of impurity Ho^{3+} ions in forsterite. Spectrometer frequencies equal 80 GHz and 170 GHz for the single ion and dimer associate, respectively. $B_0 \parallel b$, $B_1 \parallel B_0$.

The effective spin Hamiltonian

$$H = \sum_{i=1}^2 H_{\text{eff}}^i - 2JS_{z1} S_{z2} \quad (3)$$

was used to describe the field-frequency dependencies of the electron-nuclear levels of the Ho^{3+} DA. Here H_{eff}^i is the effective spin Hamiltonian (1) of a SI. The second term corresponds to the spin-spin interaction. For the DA consisting of identical ions with effective spin $S = 1/2$, four spin states may be represented as a singlet ($S = 0$) and a triplet ($S = 1$). Magnetic dipole transitions are allowed between the electron levels of the spin triplet. The parameters of the spin Hamiltonians (1) and (3), fitted for the best description of the experimental data are presented in Table 1. Corresponding theoretical dependencies are presented in Figure 3. In order to simplify the figure, only the dependencies corresponding to the hyper fine components with the same values of I_z for both ions ($I_{z1} = I_{z2}$) are presented. To determine localization of holmium ions in the crystal lattice and orientation of the principal magnetic axes, the orientation dependencies of EPR spectra were obtained at rotation of magnetic field in the crystallographic (ab) and (bc) planes. The results are presented in Figure 4.

Since in this case $g_x = g_y = 0$, these dependencies are determined by the simple expression $B_0 = B_{\text{extr}}/\cos\theta$, where B_{extr} is the minimum value of the resonance field, angle θ is the deviation of the magnetic field from the direction corresponding to this minimum value. It can be seen that there are two magnetically nonequivalent sites of SI. The corresponding principal magnetic z -axes lie in the (ab) plane and deviate from the b -axis by angles of $\pm 29^\circ$. Therefore, we can conclude that SI substitute magnesium at the M2 site. There are four magnetically nonequivalent positions of the DA. The projections of the magnetic z -axes of these centers on the (ab) plane deviate from the b -axis by the angles $\pm 29^\circ$ like in the case of the SI and deviate from the b -axis by the angles of about $\pm 4^\circ$ in the (bc) plane. The doubling of experimental points

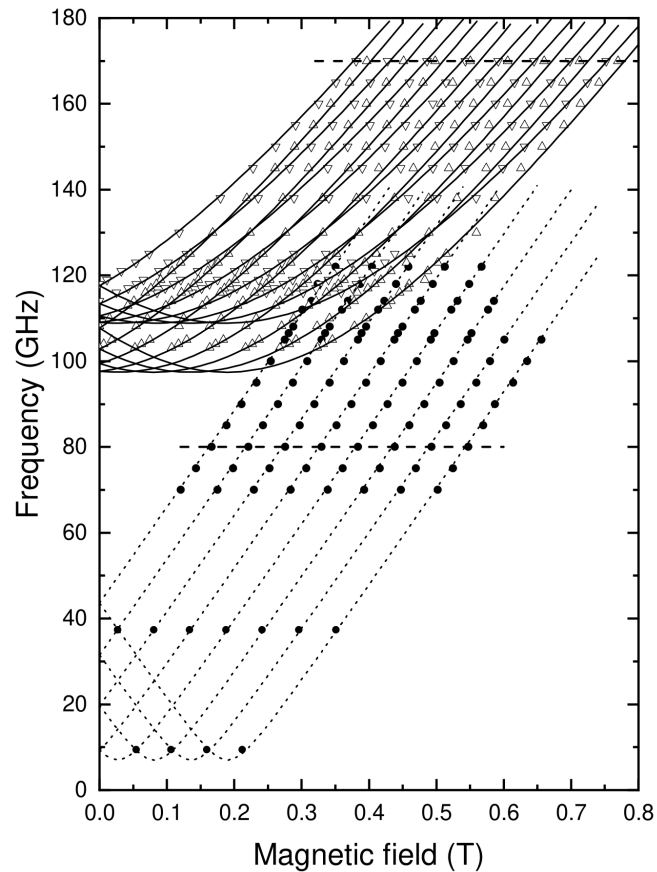


Figure 3. Field-frequencies dependencies of the HFS components of $\text{Mg}_2\text{SiO}_4:\text{Ho}^{3+}$ EPR spectra at $B \parallel b$. Circles and triangles designate experimental data for the single ion and the dimer associate, respectively. Dotted and solid lines present theoretical dependencies, calculated with spin Hamilton parameters specified in Table 1. Dashed lines indicate frequencies of measurements corresponding to the spectra in Figure 2.

in Figure 4 is due to the deviation of the axis of sample rotation from the crystallographic axis. This deviation leads to minor differences in the values of the resonance magnetic fields for the two magnetically non-equivalent centers. Angular dependencies presented in Figure 4 show that directions of the principal magnetic axes of the DA are close to that of the SI. Taking this fact into account, we suppose that the DA is formed by two Ho^{3+} ions substituting magnesium in two magnetically equivalent M2 sites. Since these M2 sites lie in the same (bc) layer, the DA consists of the two Ho^{3+} ions in the M2 sites with the Mg^{2+} vacancy in the M1 site between them. Two magnetically nonequivalent structures of these DA are highlighted in bold lines on Figure 5. The Mg^{2+} vacancy in the M1 site destroys the mirror symmetry of the crystal field in the M2 sites occupied by the Ho^{3+} ions. It results in the deviation of the principal magnetic z -axes of the DA from the (ab) plane. Fitting of the parameters of the spin Hamiltonians (1) and (3) allowed us to obtain the characteristics of the holmium impurity centers. These parameters and Euler angles θ and φ , determined orientation of the principal z -axis relative to the crystallographic axes are presented in the Table 1.

The values of energy ave an accuracy of ± 0.5 GHz for the values of Δ and ± 0.1 GHz for other parameters. The values of Euler angles are determined with an accuracy of $\pm 0.5^\circ$. The angles for the different magnetically nonequivalent centers are given in different lines. For the non-Kramers Ho^{3+} ion $g_x = g_y = 0$. Therefore, the orientation of x - and y -axes were not

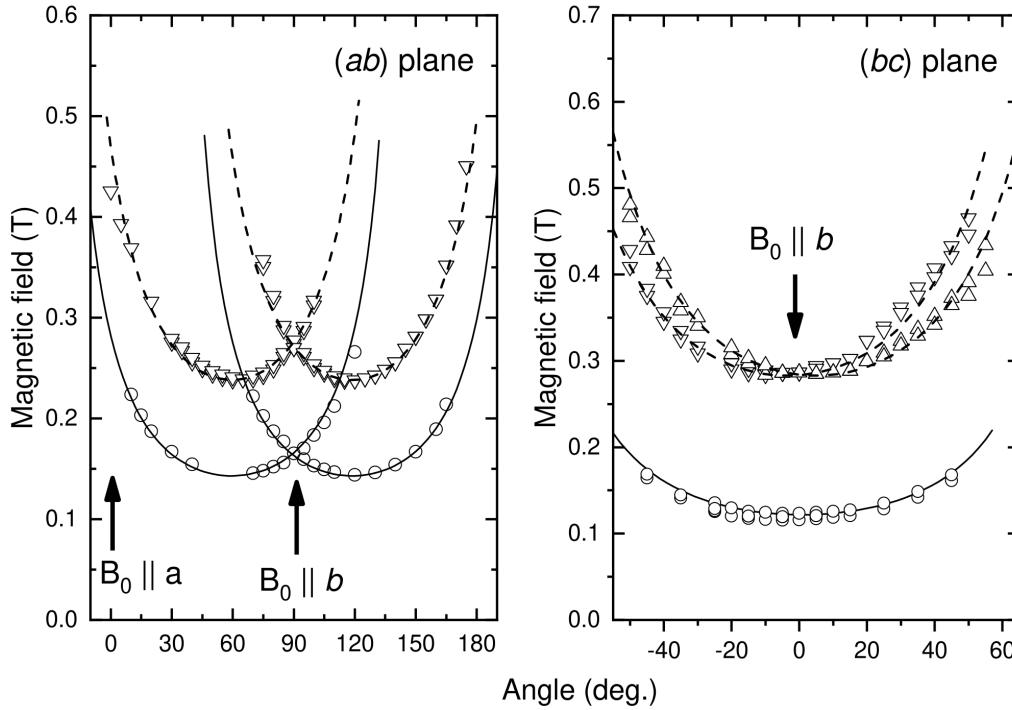


Figure 4. Angular dependencies of the lowest field lines of the HFS of the Ho^{3+} spectra in forsterite. Circles and triangles correspond to experimental data for the SI at the frequencies of 80 GHz and to the DA 140 GHz, respectively. Solid and dashed lines present functions $B_0 = B_{\text{extr}} / \cos \theta$ for the SI and DA, respectively.

Table 1. The spin-Hamiltonian parameters and Euler angles for impurity Ho^{3+} ions in forsterite.

	Δ (GHz)	g_z	A_z (GHz)	J_z (GHz)	θ (deg.)	φ (deg.)
SI(M2)	7	18.4	12.3		90	± 29
DA(M2)	103	17.9	11.8	11,4	86 94	± 29 ∓ 29

determined.

It is difficult to estimate the relative concentration of SI and DA of the Ho^{3+} ions by comparison of the intensity of the EPR spectra, since the probability of resonance transitions in this case strongly depends on the ratio between the values of the zero field splitting and the Zeeman energy. This is clearly seen in the EPR spectra of the SI ion on Figure 1. Nevertheless, comparing the spectra of the SI and DA, it can be argued that the concentration of the DA significantly exceeds the concentration of SI.

4. Tb^{3+} ions

The ground state of Tb^{3+} ion with $4f^{10}$ electron configuration is 7F_6 . The nuclear spin of ^{159}Tb (the 100% abundance) $I = 3/2$. Thus, the HFS of EPR spectra of the Tb^{3+} SI should consist of 4 “allowed” transitions. For a terbium DA, the HFS should consist of 16 “allowed” transitions. Terbium paramagnetic centers in forsterite were studied in the article [24]. Resonance transitions between electron-nuclear levels of Tb^{3+} SI and DA in forsterite were detected in the frequency range of 195–305 GHz. Left side of the Figure 6 shows the spectra of the Tb^{3+} SI substituting magnesium at the M2 sites.

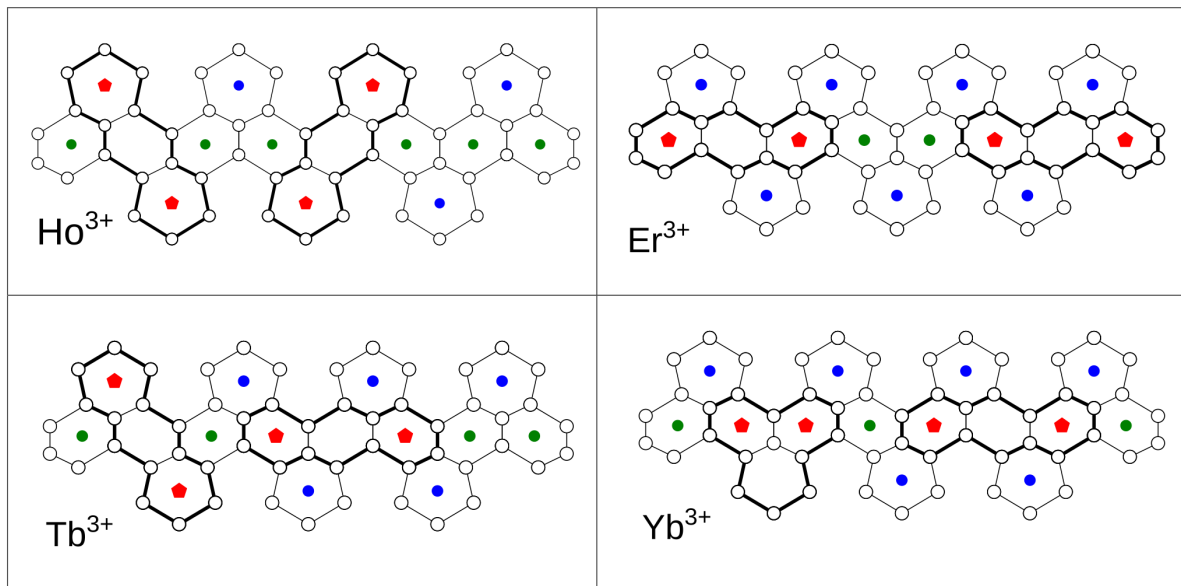


Figure 5. Structures of rare earth dimer associates in $\text{Mg}_2\text{SiO}_4:\text{Ho}^{3+}$ crystals.

It is obvious that spectra with the HFS consisting of four lines belong to the Tb^{3+} SI with nuclear spin $I = 3/2$. Measurement of the orientation dependencies of the spectra showed that the impurity ion is localized at the M2 site, and its principal magnetic z -axis is directed along the crystallographic c -axis. Therefore, there are no magnetically nonequivalent centers. The frequency-field dependencies of the spectra are well described by the effective spin Hamiltonian (1). The dashed lines show these dependencies calculated with parameters of the spin Hamiltonian presented in Table 2. At the same time, weak lines marked with asterisks can be seen on some spectra to the right of the main spectrum. These lines belong to another center. To determine the nature of the second center, we modeled the SI spectra using four Gaussians corresponding to the expected hyper fine structure of the single Tb^{3+} ion. The simulated spectra were then subtracted from the experimental spectra. Figure 7 shows an example of this procedure. Frequency-field dependencies of the residual spectra obtained after this treatment are shown in the right part of Figure 6.

Table 2. The spin-Hamiltonian parameters and Euler angles for impurity Tb^{3+} ions in forsterite.

	Δ (GHz)	g_z	A_z (GHz)	J_z (GHz)	θ (deg.)	φ (deg.)
SI(M1)	236	15.9	5.5		75	± 12
					105	± 12
DA(M1)	259	16.0	5.8	-6.8	74	± 12
					106	± 12
SI(M2)	195	15.8	5.4		0	0
DA(M2)	194	16.0	6.0	-6.8	2	± 2

Obviously, the residual spectra do not belong to the Tb^{3+} SI, for which the HFS should consist of four lines. Therefore, we assume that these spectra belong to the DA of two Tb^{3+} ions. Each transition between electron levels should consist of 16 "allowed" transitions. The lines of these transitions overlap each other, forming complex irregular spectra, which are seen in Figure 6 and Figure 7.

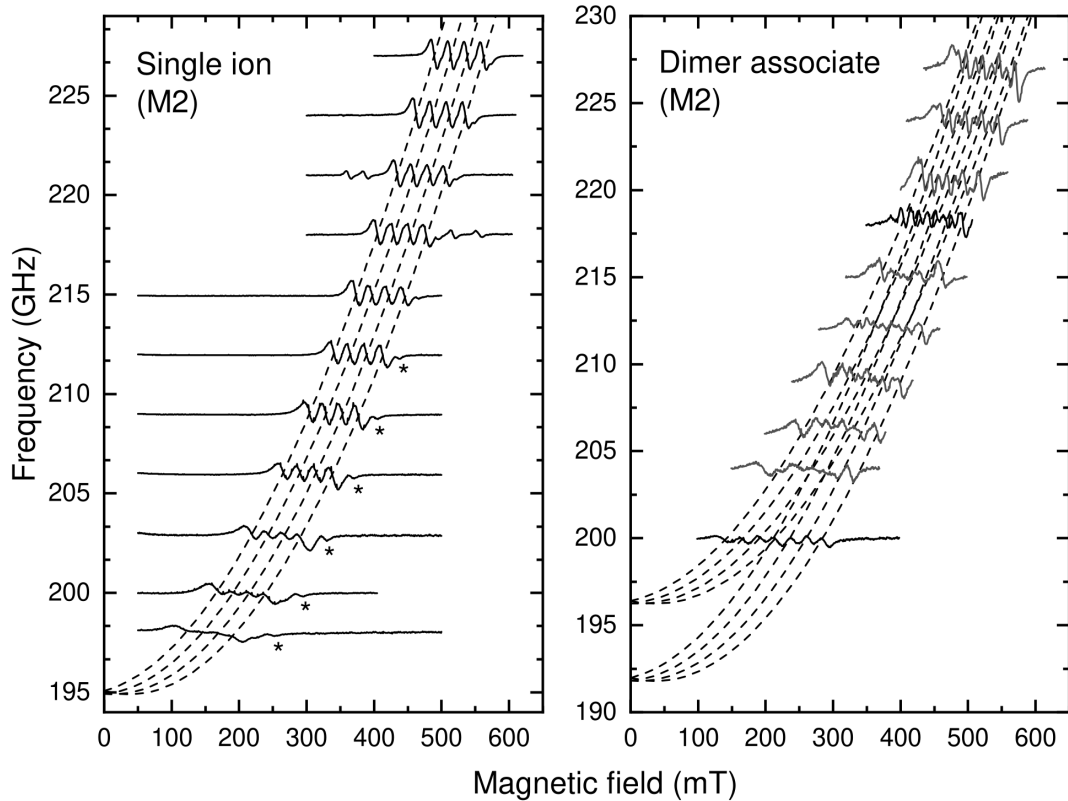


Figure 6. EPR spectra of the Tb^{3+} ions the M2 site of forsterite recorded at various frequencies, corresponding to the positions of the spectra baselines on the y -axis. $B_0 \parallel c$ -axis, $T = 4.2$ K. Lines present calculated frequency-field dependencies of resonance transitions for the several hyperfine components of the single ions and dimer associates.

Parameters of the Hamiltonian (3) corresponding to the best fit of the calculated dependencies and experimental results are presented in Table 2. It is seen that the values of these parameters are very close to those of the SI. Orientation dependencies of the highest-field hyperfine component of the center 2 marked by asterisks in Figure 1 indicate the presence of two magnetically nonequivalent centers with principal magnetic axes deviated from the crystal c -axis by angles of $\pm 1.5^\circ$ in the (bc) -plane. The projections of the principal magnetic axes on the (ac) plane coincide with the c -axis. It is very close to the orientation of the z -axis of the SI. Therefore, we assure that this DA is formed by two Tb^{3+} ions situated in the nearby M2 sites, and there is a disturbing factor violating the mirror symmetry of the M2 site in the (bc) plane. A satisfactory theoretical description of the experimental frequency-field dependencies has been obtained for the case when the greatest contribution to the experimental spectra is made by two transitions between electron levels belonging to the state $S = 1$. The dashed and dotted lines on right part of Figure 6 shows part of the theoretical dependencies corresponding to transitions between hyperfine components with the same projections of the I_z nuclear spins for both ions.

Resonance transitions belonging to another Tb^{3+} impurity centers were found in the frequency range of 235–300 GHz. The spectra of these centers recorded at different frequencies are shown on Figure 8.

Lines present theoretical dependencies calculated with parameters of spin Hamiltonians (1) and (3) presented in Table 2. The orientation dependencies of these transitions have shown that the principal magnetic z -axes are deviated from the (ab) and (bc) planes. That is, the Tb^{3+} ions substitute magnesium at the M1 sites.

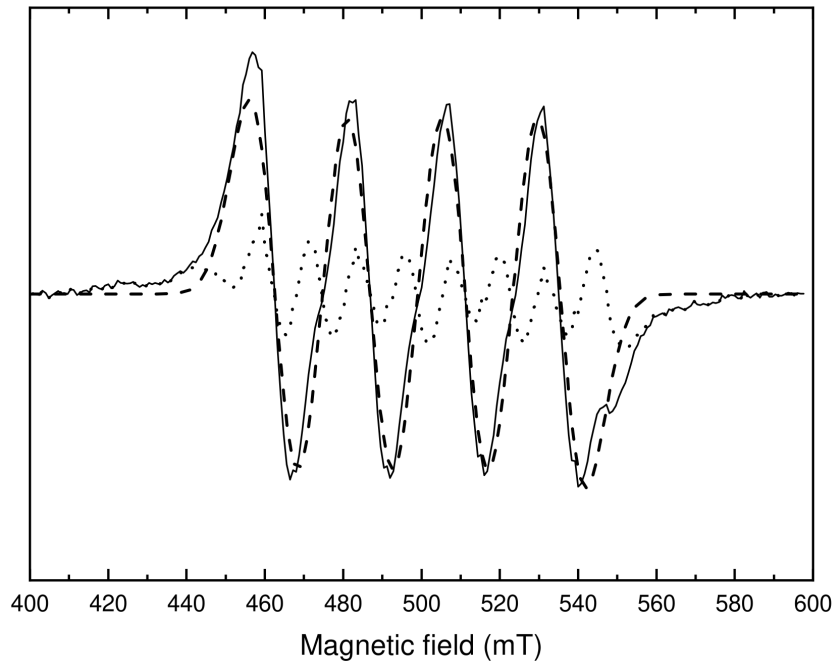


Figure 7. Decomposition of the experimental spectrum of the Tb^{3+} ions at $\nu = 224$ GHz into spectra of SI and DA. $T = 4.2$ K. Solid, dashed, and dash-dotted lines are the experimental spectrum, the calculated spectrum of the SI and residual spectrum of a DA, respectively.

Structures of the Tb^{3+} dimer associates are shown in Figure 5. Orientations of the z -axes and parameters of the spin Hamiltonians for all Tb^{3+} centers are presented in Table 2 .

5. Er^{3+} ions

The ground state of Er^{3+} ion with the electron $4f^{11}$ configuration is $^4I_{15/2}$. EPR spectra of Er^{3+} ions with a natural isotope content should contain a line of even isotopes with zero nuclear spin and lines of the ^{167}Er isotope with nuclear spin $= 7/2$. The natural content of ^{167}Er is about 23%, so the relative intensity of the HFS of this isotope is about 0.029. Erbium paramagnetic centers in forsterite were studied in the article [25]. Resonance transitions were identified as spectra of SI and DA of Er^{3+} ions substituting magnesium at the M1 sites. This follows from the orientation dependencies of the spectra shown on Figure 9, where extremes of these dependencies do not coincide with the crystallographic axes.

It can be seen that there are two groups of resonance transitions consisting of three lines each. The orientation dependencies for these groups are mirror-symmetric with respect to the directions of the crystallographic a - and b -axes. The Er^{3+} ion in the ground state has a total electron magnetic moment $S = 15/2$. So it is a Kramers ion with at least twofold degenerated electron Stark levels at zero magnetic field. Three different resonance lines in each group may correspond to three different erbium centers with different values of the effective g -factors. In this case, a change of the spectrometer frequency should lead to the proportional change in the splitting between the resonance lines on the EPR spectra. The second possibility is the formation of DA, which include two erbium ions connected by spin-spin interaction. Such DA has one singlet electron level with a total magnetic moment $S = 0$ and a triplet state with $S = 1$. If there is a nonzero term $D(S_z)^2$ in the spin Hamiltonian describing the spin-spin interaction, the nonzero splitting Δ appears between the electron states $S_z = 0$ and $S_z = \pm 1$. In thin case, the splitting between two lines in the spectra is determined by Δ and it is not changed with

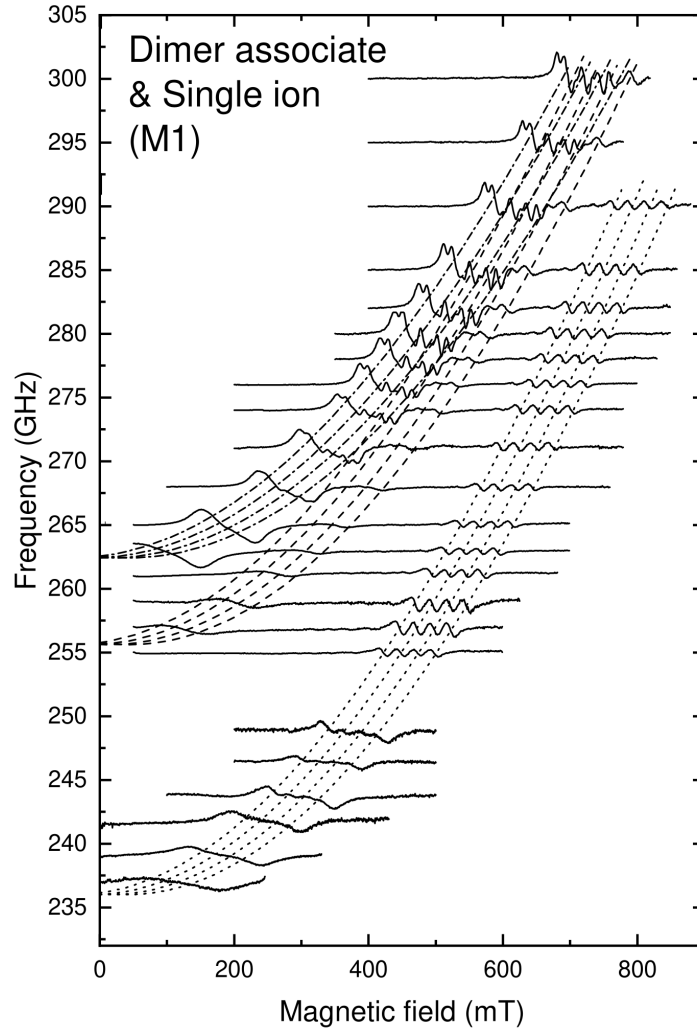


Figure 8. EPR spectra of the Tb^{3+} ions in the M1 site of forsterite recorded at various frequencies, corresponding to the positions of the spectra baselines on the y -axis. $B_0 \parallel c$ -axis, $T = 4.2$ K. Lines present calculated frequency-field dependencies of resonance transitions for the several hyperfine components of the single ions and dimer associates.

change of spectrometer frequency. Two spectra of Er^{3+} ions in forsterite recorded in X- and Q-bands are presented in Figure 10.

It can be seen that increase in the spectrometer frequency three times only slightly changes the distance between the resonance lines in the spectra. Therefore, it can be concluded that one line (middle) on spectra belongs to the Er^{3+} SI, and two extreme lines belong to the Er^{3+} DA. The resonance lines of the SI and DA have approximately the same intensity. This means that the concentrations of these paramagnetic centers are comparable. Measurements of the orientation dependencies of the spectra in three crystallographic planes made it possible to determine magnetic parameters of the Er^{3+} impurity centers in forsterite. The simple spin Hamiltonian for effective spin $S = 1/2$

$$H_i = \mu_B \mathbf{B} \cdot \mathbf{g} \cdot \mathbf{S} \quad (4)$$

was used for the SI, and the spin Hamiltonian

$$H = H_1 + H_2 + \mathbf{S}_1 \cdot \mathbf{A} \cdot \mathbf{S}_2 \quad (5)$$

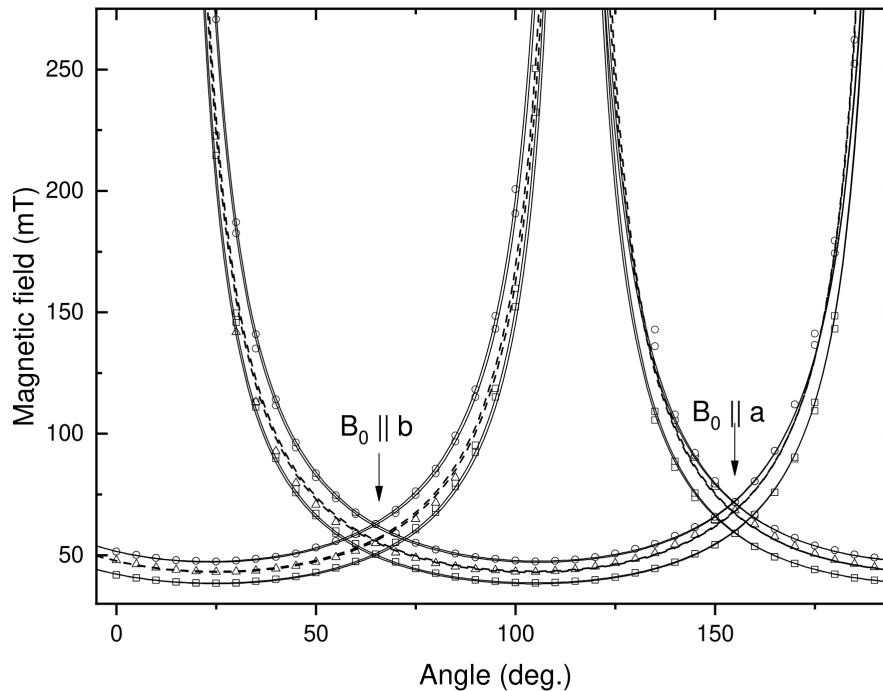


Figure 9. Orientation dependencies of resonance transitions of the Er^{3+} ions at rotation of magnetic field in the (ab) plane. $\nu = 9.386$ GHz. Circles and squares correspond to the experimental data for the DA, triangles correspond to the SI. Lines present results of calculations with parameters presented in Table 3.

was used for the DA.

The best agreement between the experimental and calculated data was obtained with the parameters presented in Table 3. It can be seen that the magnetic properties of all the centers are characterized by strong anisotropy, close to one-dimensional magnetism of the Ising type. For SI and DA, the principal magnetic z -axes of the four magnetically nonequivalent centers are deviated from the (ab) plane by the angles of $\pm 6.2^\circ$ and $\pm 7.5^\circ$, respectively, and their projections onto the (ab) plane deviate from the a -axis by the angles of $\pm 54^\circ$ and $\pm 51^\circ$, respectively. As well as $g_x = g_y = 0$ for the Yb^{3+} DA, the angles ψ are not presented in Table 3.

Table 3. The spin-Hamiltonian parameters and Euler angles for impurity Er^{3+} ions in forsterite.

	g_x	g_y	g_z	J_x (GHz)	J_y (GHz)	J_z (GHz)	θ (deg.)	φ (deg.)	ψ (deg.)
SI(M1)	0	1.2	15.6				84	± 36	∓ 55
							96	± 36	∓ 55
DA(M1)	0	0	15.6	0	0	2.78	82	± 40	
							96	± 36	

The structures of two Er^{3+} DA with the mirror-symmetric magnetic z -axes are presented in Figure 5.

6. Yb^{3+} ions

The ground state of Yb^{3+} ion with the electron $4f^{13}$ configuration is $^2F_{7/2}$. The EPR spectra of Yb^{3+} ions with a natural isotope content contain a strong line due to even isotopes with zero nuclear spin and weak lines of odd isotopes ^{171}Yb , with nuclear spin $I = 1/2$ and ^{173}Yb with

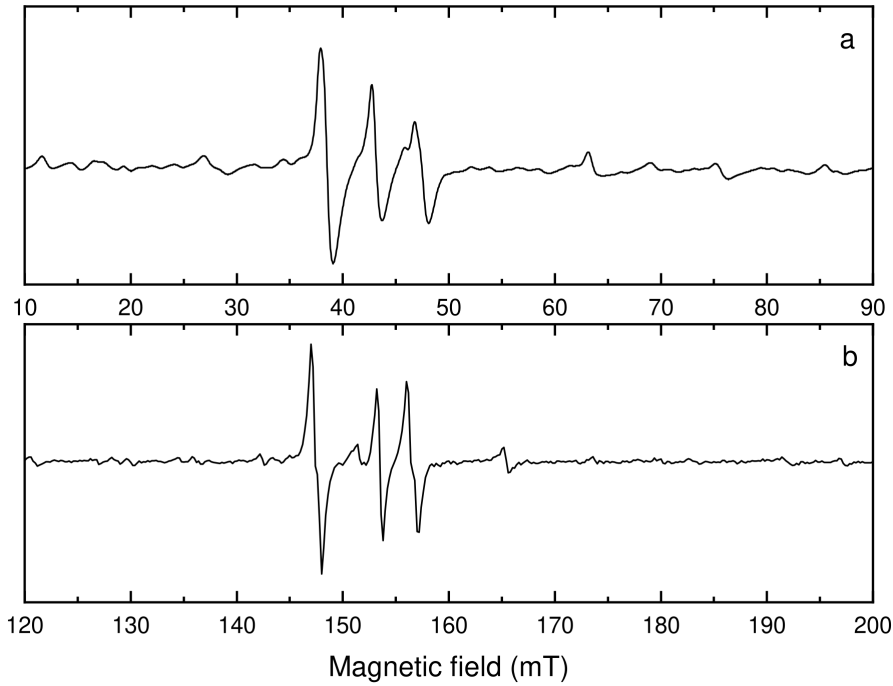


Figure 10. Spectra of the Er^{3+} ions in synthetic forsterite, recorded at different frequencies. Orientation of magnetic field corresponds to the minimal values of the resonance magnetic field in Figure 9 (110°). a - $\nu = 9.378$ GHz, b - $\nu = 33.93$ GHz.

nuclear spin $I = 5/2$. Natural contents of the ^{171}Yb and ^{173}Yb isotopes are 14.3% and 16.13%, respectively. Therefore, the relative intensities of the HFS lines of these isotopes are about 0.1 and 0.04. Ytterbium paramagnetic centers in forsterite were studied in the articles [26,27]. Figure 11 shows the orientation dependence of the spectra at rotation of the magnetic field in the (ab) plane.

It can be seen that there are 3 groups of lines on the spectra. The groups denoted M1(1) and M1(2) have orientation dependencies characteristic for impurity ions substituting magnesium at the M1 sites. The middle pair of lines in each group corresponds to magnetically nonequivalent Yb^{3+} SI at the M1 site. The extreme, more intensive pairs of lines correspond to magnetically nonequivalent DA. The M2 group of lines has an orientation dependence characteristic for the single ion at the M2 site. The measurement of the orientation dependencies of the spectra in three crystallographic planes made it possible to determine the characteristics of all paramagnetic centers. Results are presented in Table 4. It is seen that $g_x, g_y \gg g_z$. It means that with an arbitrary orientation of the external magnetic field, the magnetic moments of the Yb^{3+} ions lie close to the (xy) plane. This corresponds to a strong anisotropy of the magnetic properties of the easy-plane type. Various signs of the principal values of the \mathbf{J} -tensor indicate that the spin-spin interaction between Yb ions in the DA has a predominantly magnetic dipole-dipole origin.

It is quite strange that for the Yb^{3+} ions in the M1 and M2 groups of lines, the principal values of the \mathbf{g} -tensor are almost the same. This means that the eigen functions of the ground doublets of Yb^{3+} ions in these groups are also almost the same. Moreover, as can be seen in Figure 12, the orientation dependencies of the resonance transitions under rotation around the c -axis are very close also. This prompted us to conclude that the paramagnetic center with the orientation dependency characteristic for the M2 site is actually the DA of the Yb^{3+} ions in the M1 sites with a magnesium vacancy in the neighboring M2 site. Due to the strong

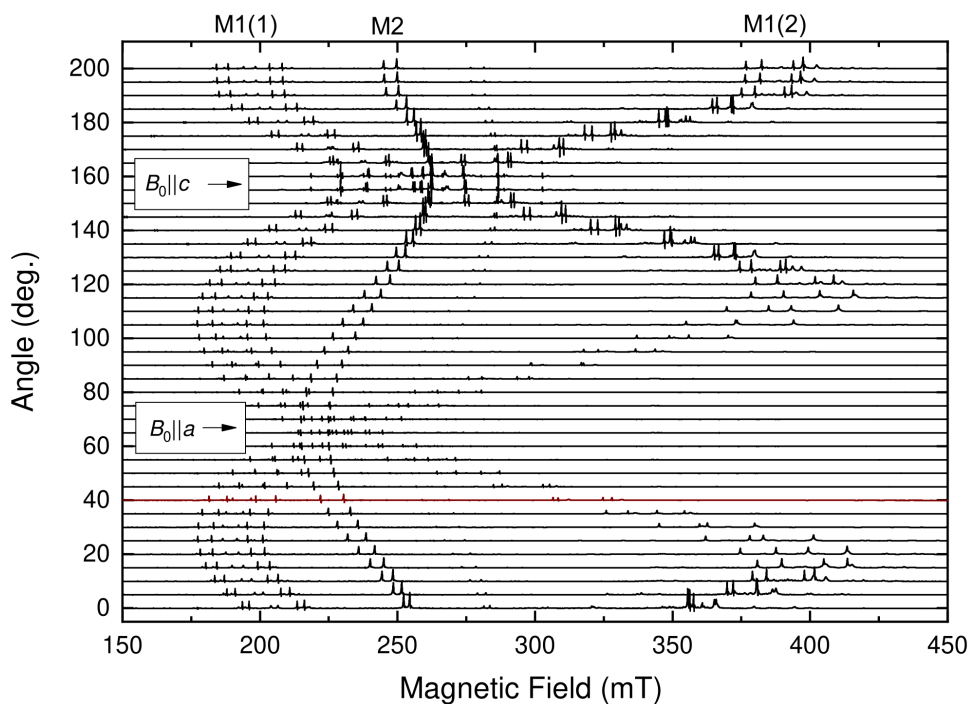


Figure 11. EPR spectra of Yb^{3+} ions in forsterite under rotation of the magnetic field in the ac plane. The position of the spectra along the ordinate axis corresponds to the orientation of the magnetic field. The spectrometer frequency $\nu = 9.723$ GHz.

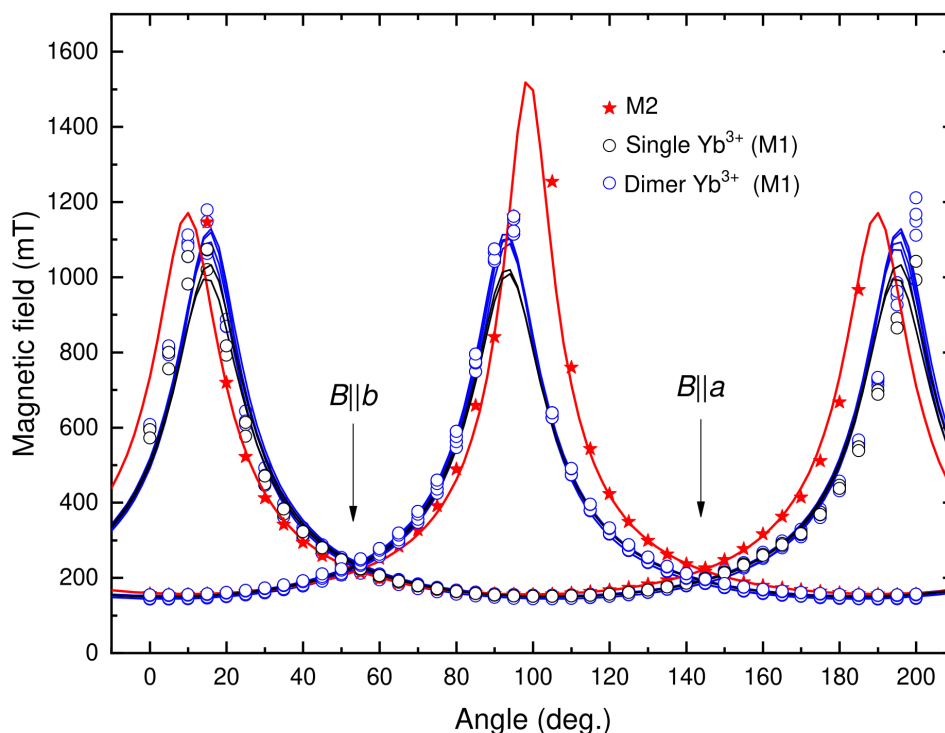


Figure 12. Dependencies of the resonance values of external magnetic field on the magnetic field orientation in the crystallographic (ab) plane. Black, blue and red icons present experimental data for the the SI(M1) and M2 centers, respectively. Lines present calculations with the spin Hamiltonian (4) and (5) for the SI and DA, respectively.

exchange interaction between closely spaced Yb^{3+} ions, they lost their independence and become a single paramagnetic center with the mirror symmetry plane perpendicular to the c -axis. In this case, the orientation dependencies of the EPR spectra should be similar to that for the single paramagnetic center located at the M2 site. A very high probability of the formation of such dimers was confirmed by calculations performed in the article [28].

It is known that, in some cases, the value of spin of a paramagnetic center can be determined by the measurement of the frequency of transient nutation of S_z spin component under intensive resonance excitation. For the resonance transition with a change on the magnetic quantum number $\Delta m_s = \pm 1$, the frequency of nutation is determined by the expression [29]

$$\nu(m_s, m_s + 1) = \nu_R \sqrt{S(S + 1) - m_s(m_s + 1)}. \quad (6)$$

Here $\nu_R = g\mu_B B_1/h$ - the Rabi frequency for spin $S = 1/2$, S is the total effective electron spin of the paramagnetic center ($S = 1/2$ for the SI and $S = 1$ for the DA), m_s is the projection of the electron spin onto the quantization axis, B_1 is the amplitude of the magnetic component of the microwave field. To observe transient nutations, we used a three-pulse sequence. The first pulse of variable duration (t) was followed by the two-pulse sequence of the Hahn primary echo. The results of measurements are shown in Figure 13

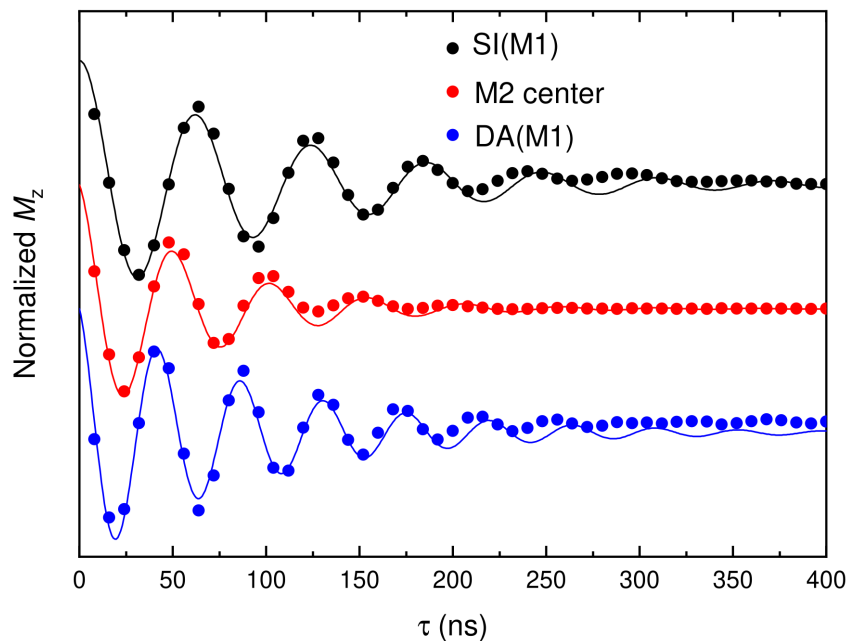


Figure 13. Dependencies of the amplitude of the two-pulse spin echo on duration of the previous resonance microwave pulse for Yb^{3+} ions in forsterite. The black, blue and red circles correspond to experimental data for the SI(M1), DA(M1) and M2 center, respectively. The lines are approximations of experimental data by exponentially decaying cosines.

The frequencies of nutation were 16.2 MHz, 22.4 MHz and 19.2 MHz, for the Yb^{3+} SI and DA of ions at the M1 sites, and the center M2, respectively. According to expression (6), the theoretical ratio of the nutation frequencies for the DA and the SI should be $\sqrt{2} \approx 1.41$. The measured ratio is about 1.38. This is very close to the theoretical ratio. The value of the nutation frequency for the M2 center is between the frequency values of the Yb^{3+} SI and DA. An explanation for this can be given based on the results obtained in the article [30]. It was shown in this article that if two paramagnetic centers with spin $S = 1/2$ are connected by an

isotropic exchange interaction and two resonance transitions between the states $S_z = 0$ and $S_z = \pm 1$ are excited with the same frequency, the nutation frequency equals to ν_R . If, as a result of the anisotropic part of the spin-spin interaction, a splitting appears between the states $S_z = 0$ and $S_z = \pm 1$, and the only resonance transition is excited, then the nutation frequency equals $\sqrt{2}\nu_R$. These cases are realized for the DA of the Yb^{3+} ions at the M1 sites. If both resonance transitions are excited at different frequencies, two different frequencies will be present in the signal of transient nutation. Interference of these oscillations can give a visible effect of an intermediate nutation frequency (6). We believe that the intermediate nutation frequency of the M2 center is explained by strong isotropic exchange interaction between the Yb^{3+} ions and presence of a dipole-dipole interaction. Therefore, it can be argued that the M2 center is the dimer associate of the Yb^{3+} ions substituting magnesium at two mirror-symmetrical M1 sites located nearby. The magnesium vacancy in this case is localized in the nearby M2 site. The structure of the Yb^{3+} DA is highlighted on Figure 5.

Table 4. The spin-Hamiltonian parameters and Euler angles of impurity Yb^{3+} ions in forsterite.

	g_x	g_y	g_z	J_x (GHz)	J_y (GHz)	J_z (GHz)	θ (deg.)	φ (deg.)	ψ (deg.)
SI(M1)	4.9	2.0	0.6				82	± 36	± 23
							98	± 36	± 23
DA(M1)	5.0	2.1	0.6	0	0.6	-0.8	83	± 37	± 23
							97	± 37	± 23
M2 center	4.5	2.6	0.3				90	± 45	0

7. Summary

Paramagnetic centers formed by impurity rare earth ions Ho^{3+} , Tb^{3+} , Er^{3+} and Yb^{3+} ions in single crystals of synthetic forsterite (Mg_2SiO_4) were studied by multi-frequency EPR spectroscopy in the frequency range of 9.5–300 GHz. It is shown that impurity ions substitute magnesium in oxygen octahedra both in the form of single ions with non-local compensation of excess cation charge arising at the heterovalent substitution of divalent magnesium ions with trivalent impurity ions and in the form of dimer associates formed by two closely spaced trivalent impurity ions with the associated magnesium vacancy, which plays the role of a local charge compensator. It is shown that the concentration of the dimer associates is several orders of magnitude higher than the concentration expected with a statistically uniform distribution of impurity ions in the crystal lattice. Localization of the impurity ions in the crystal lattice, the structure of the dimer associates, and the magnetic properties of all detected impurity centers are determined.

Acknowledgments

I am grateful to Prof. B.Z. Malkin for attracting our attention to the effect of dimer self-organization of impurity trivalent ions substituting divalent ions in quasi-one-dimensional structural chains in single crystals.

I would like to thank my colleagues, together with whom the described results were obtained.

E.V. Zharikov, K.A. Subbotin, and D.A. Lis from Prokhorov General Physics Institute of RAS grew the samples for the research.

V.A. Shustov from Zavoisky Physical-Technical Institute has done a lot of work for the determinations of crystallographic axes in samples by the X-ray diffraction.

A.A. Konovalov, L.V. Mingalieva, A.A. Sukhanov R.B. Zaripov from Zavoisky Physical-Technical Institute and S.I. Nikitin, E.N. Vorobieva, D.G. Zverev from Kazan (Volga Region) Federal University carried out measurements of the EPR spectra. Part of measurements was carried out using facilities of the Distributed Spectral-Analytical Center of Shared Facilities for Study of Structure, Composition and Properties of Substances and Materials of FRC Kazan Scientific Center of RAS.

V.B. Dudnikova from Moscow State University carried out numerical modeling of various variants of the dimer associate structures in order to determine relative probabilities of their formation.

The work was performed with the financial support from the government assignment for FRC Kazan Scientific Center of RAS.

References

1. Ohlsson N., Mohan R. K., Kröll R. K. *Opt. Commun.* **201**, 71 (2002).
2. Luis F., Repolles A, Martinez-Perez M. J., Aguila D., Roubeau O., Zueco D., Alonso P.J., Evangelisti M., Camon A., Sese J., Barrios L. A., Aromi G. *Phys. Rev. Lett.* **107**, 117203 (2011).
3. McPherson G. L., Henling L. M. *Phys. Rev. B* **16**, 1889 (1977).
4. Henling L. M., McPherson G. L. *Phys. Rev. B* **16**, 4756 (1977).
5. Berdowski P. A. M., Lammers M. J. J., Blasse G. *J. Chem. Phys.* **83**, 476 (1985).
6. Barthem R. B., Buisson R., Cone R. L. *J. Chem. Phys.* **91**, 627 (1989).
7. Barthou C., Barthem R. B. *J. Lumin.* **46**, 9 (1990).
8. Cockroft N. J., Jones G. D., Syme R. W. G. *J. Lumin.* **43**, 275 (1989).
9. McPherson G. L., Meyerson S. L. *Chem. Phys. Letters* **167**, 471 (1990).
10. Mujaji M., Jones G. D., Syme R. W. G. *Phys. Rev. B* **48**, 710 (1993).
11. Malkin B. Z., Leushin A. M., Heber J., Altwein M., Moller K., Fazlizhanov I. I., Ulanov V. A. *Phys. Rev. B* **62**, 7063 (2000).
12. Mehta V., Gourier D. *J. Phys.: Condens. Matter* **13**, 4567 (2001).
13. Tarasov V. F., Shakurov G. S., Malkin B. Z., Iskhakova A. I., Heber J., Altwein M. *JETP Lett.* **65**, 559 (1997).
14. Malkin B. Z., Iskhakova A. I., Tarasov V. F., Shakurov G. S., Heber J., Altwein M. *J. Alloys & Compounds* **275-277**, 209 (1998).
15. Tarasov V. F., Shakurov G. S. *Appl. Magn. Reson.* **2**, 571 (1991).
16. Shakurov G. S., Tarasov V. F. *Appl. Magn. Reson.* **21**, 597 (2001).
17. Apreleva A. S., Sukhanov A. A., Tarasov V. F., Subbotin K. A., Zharikov E. V. *Magn. Reson. Solids* **21**, 19402 (2019).
18. Birlle J. D., Gibbs G. V., Moore P. B., Smith J. V. *The Amer. Mineralog.* **53**, 807 (1968).
19. Dudnikova V. B., Urusov V. S., Zharikov E. V. *Inorg. Mater.* **41**, 627 (2005).
20. Gaister A. V., Zharikov E. V., Konovalov A. A., Subbotin K. A., Tarasov V. F. *JETP Lett.* **77**, 625 (2003).

21. Konovalov A. A., Lis D. A., Malkin B. Z., Nikitin S. I., Subbotin K. A., Tarasov V. F., Vorobieva E. N., Zharikov E. V., Zverev D. G. *Appl. Magn. Reson.* **28**, 267 (2005).
22. Griffith J. S. *Phys. Rev.* **132**, 316 (1963).
23. Baker J. M., Hutchison C. A. Jr, Martineau P. M. *Proc. R. Soc. Lond.* **A 403**, 221 (1986).
24. Konovalov A. A., Lis D. A., Subbotin K. A., Tarasov V. F., Zharikov E. V. *Appl. Magn. Reson.* **45**, 193 (2014).
25. Zaripov R. B., Mingalieva L. V., Tarasov V. F., Zharikov E. V., Subbotin K.A., Lis D.A. *Physics of the Solid State* **61**, 174 (2019).
26. Tarasov V. F., Sukhanov A. A., Dudnikova V. B., Zharikov E. V., Lis D. A., Subbotin K. A. *JETP Lett.* **106**, 92 (2017).
27. Tarasov V. F., Sukhanov A. A., Zharikov E. V., Subbotin K. A., Lis D. A. *Appl. Magn. Reson.* **53**, 1211 (2022).
28. Dudnikova V. B., Zharikov E. V. Lis D. A., Eremin N. N. *Phys. Solid State* **61**, 614 (2019).
29. Schweiger A., Jeschke G. *Principles of Pulse Electron Paramagnetic Resonance* (Oxford University Press , N.Y. 2001), 429 p.
30. Salikhov K. M. *JETP* **135**, 617 (2022).